REFERENCE

IC/82/146
INTERNAL REPORT
(Limited distribution)

International Atomic Energy Agency
and
United Nations Educational Scientific and Cultural Organization

INTERNATIONAL CENTRE FOR THEORETICAL PHYSICS

ELECTRON DISTRIBUTIONS OF THE FIRST-ROW HOMONUCLEAR DIATOMIC MOLECULES, A_2 *

Bayani I. Ramirez
International Centre for Theoretical physics, Trieste, Italy, **
and
Fakultät für Chemie, Universität Bielefeld, 4800 Bielefeld 1, West Germany.

ABSTRACT

Electron momentum density contour maps of the first-row homonuclear diatomic molecules, A_2, are obtained from near Hartree-Fock wave functions. Both the total momentum density and momentum density difference (molecule - isolated atoms) maps present trends that may be related to the binding in the molecules. These results are compared with the corresponding charge density maps in position space (Bader, Henneker and Cade 1967).

MIRAMARE - TRIESTE
August 1982

* To be submitted for publication.

** Present address.

1. INTRODUCTION

In previous papers the explicit characteristics of electron momentum density (EMD) maps were used to interpret trends in the chemical binding of the first-row diatomic hydrides, AH, (Ramirez 1982a), and to contrast the formation of the bound state of molecular hydrogen, H_2, with the unbound molecule of helium, He_2, (Ramirez 1982b). Similar studies in momentum space ($\tilde{p}$-space) have been done by Henneker and Cade (1968) on lithium fluoride, LiF, and nitrogen, N_2, to compare what are basically ionic and covalent molecules, respectively. Although some work has been done relating chemical binding to directional Compton profiles and Compton profile anisotropies (Kaijser and Smith 1976, Matcha and Pettitt 1979), two-dimensional EMD maps offer a more direct study of chemical binding in $\tilde{p}$-space, aside from providing a complementary view of the position space ($\tilde{x}$-space) charge density maps of the same systems; this is because charge and momentum densities weigh most importantly opposite regions of space.

The EMD distributions of the first-row diatomic hydrides (Ramirez 1982a) confirmed the "bond directional principle" (Epstein and Tanner 1977) which states that in a chemical bond the linear momentum of an electron is more likely to be directed normal to, rather than along the bond axis. The total EMD maps of the molecules AH showed how this likelihood increased as the molecule became more tightly bound in the forward sequence LiH → HF. On the other hand, the EMD maps of H_2 and He_2 demonstrated that He_2 is unbound precisely because its electrons are more likely to move parallel to, rather than perpendicular to the diatomic axis, thereby contradicting

the "bond directional principle". This effort is continued in this paper for the ground states of the first-row homonuclear diatomics, A_2, one of whose members, Be_2, is unbound. Thus, the conclusions derived in the first two papers can be fully tested in this series of molecules, whose charge density maps have been studied by Bader, Henneker and Cade (1967), hereafter referred to as BHC.

If the ground state of a system can be expressed as a single Slater determinant, its total momentum density is given by

$$\rho(\tilde{p}) = \sum_i \rho_i(\tilde{p}) \qquad (1)$$

where $\rho_i(\tilde{p})$ is the EMD of the i th electron, obtained from the Fourier-Dirac transform of its $\tilde{r}$-space molecular orbital (MO). Figures 1 and 3 show the total EMD distributions of the molecules A_2 as contour maps on a two-dimensional plane in $\tilde{p}$-space that includes the origin and with p_z parallel to the diatomic axis. Note that $\rho(\tilde{p})$ is symmetric with respect to both axes and that the three-dimensional distribution may be obtained by rotating the given map about the p_z-axis.

Momentum density difference (molecule-isolated atoms) maps for the molecules A_2 (Figures 2 and 3) are obtained through the formula

$$\Delta\rho(\tilde{p}) = \rho_{A_2}(\tilde{p}) - 2\rho_A(\tilde{p}) \qquad (2)$$

where ρ_{A_2} and ρ_A are the molecular and atomic momentum densities, respectively. The solid contour lines and the dash-dot contour

lines indicate regions of increased and reduced momentum densities, respectively, in the molecule vis-a-vis the isolated atoms.

Table 1 gives the value at the origin of the total EMD and density difference for the first-row homonuclear diatomic molecules.

The molecular wavefunctions used (Cade and Wahl 1974) are alleged to be very close approximations to the true Hartree-Fock wavefunctions; these results are for the $Li_2(X'\Sigma_g^+)$, $Be_2(\ ^1\Sigma_g^+\ )$, $B_2(X^3\Sigma_g^-)$, $C_2(X'\Sigma_g^+)$, $N_2(X'\Sigma_g^+)$, $O_2(X^3\Sigma_g^-)$, and $F_2(X'\Sigma_g^+)$ at their equilibrium separation (for Be_2, R=3.5 bohr). Atomic wavefunctions of near Hartree-Fock quality (Clementi and Roetti 1974) were used to obtain the atomic momentum densities. In calculating $\Delta\rho$ non-spherical atomic densities were subtracted from the molecular densities; however, the atomic configuration is always made consistent with that in the molecule (BHC).

2. DISCUSSION OF MAPS

2.1 The Total Molecular Momentum Density

The total EMD contour maps (Figure 1) of the bound members of the first-row homonuclear diatomic molecules (Li_2, B_2, C_2, N_2, O_2, and F_2) reveal that the molecule A_2 becomes relatively more tightly bound as atom A goes from Li $\longrightarrow$ F. BHC have related the tightness of of the binding in a molecule to the narrowness of its charge density; in $\tilde{p}$-space, a narrow charge density becomes a broad momentum density. Thus, F_2, which has a more spreadout EMD than say, N_2, is more tightly bound than the latter. These maps should be compared to their counterparts in $\tilde{x}$-space (Figure 1 of BHC).

The shape of the total EMD maps support the "bond directional principle" of chemical binding. In going from $Li_2 \longrightarrow F_2$ there is a definite trend for the contours to be more elongated along the vertical or p_x-axis, i.e., normal to the bonding direction, which proves that with the increasing tightness of the chemical bond, the electronic momentum $\tilde{p}$ is more likely to be directed perpendicular to, rather than parallel to the diatomic axis.

Figure 1 therefore clearly shows that as the relative tightness of the binding of the molecule A_2 increases, its EMD broadens, but in such a manner that the electron momentum $\tilde{p}$ has $p_x > p_z$. The decreasing value of the total EMD at the origin (as given in Table 1) also shows that the distribution is becoming more spreadout in the forward sequence.

2.2 The Momentum Density Difference Distribution

To see how the electronic momentum is redistributed upon molecular formation, relative to the isolated atoms, the momentum density difference maps (molecule-isolated atoms) of the first-row homonuclear diatomic molecules (except for Be_2) are plotted in Figure 2. This should be compared with the complementary charge density maps of the same molecules, shown in Figure 3 of BHC. Figure 2 shows dramatically what happens in momentum space when two similar atoms A combine to form the molecule A_2. In general, there is a negative density difference or depletion region at low momenta (indicated by the dash-dot contours around the origin), and positive $\Delta\rho$ regions at higher momentum. Thus, the electrons of the molecule A_2 have a larger probability of being in high momentum states, than the electrons of two isolated A atoms. Li_2 is an exception because it has a positive $\Delta\rho$ region, instead of a depletion region around the origin, but this increase in density at low-$\tilde{p}$ is balanced by the two disk-like depletion regions at $p_z \simeq 0.2$ a.u. The density difference maps thus confirm what has been stated in regard to the total EMD maps: the more tightly bound is the molecule A_2, the greater is the probability that its electrons will have higher momentum, relative to two isolated atoms A.

It is much more difficult to see a trend in bonding in the homonuclear diatomics A_2, in comparison with the first-row diatomic hydrides AH, because in AH the bonding can be localized to the electron shared by H with atom A, while in A_2 a variety of bonds can be present. For example, B_2 and C_2 possess one and two

pi bonds, respectively, according to molecular-orbital theory, while Li_2 is basically s-bonded. Thus, the density difference map of Li_2 is very different from that of B_2 and C_2 in the disposition of its positive and negative $\Delta\rho$ regions. Note however that C_2's $\Delta\rho$ map is approximately twice that of B_2. N_2, O_2 and F_2 all possess one bond of $p\sigma$-character and two, one and zero pi bonds, respectively. Thus, there is a noticeable change in the $\Delta\rho$ map from C_2 to N_2. The last three maps show the influence of the pi bonds on the density difference maps of these molecules.

2.3 The Unbound Molecule Be_2

The total EMD and density difference maps of Be_2 — the only unbound member of the first-row homonuclear diatomic molecules — are plotted in Figure 3. This should be compared with the corresponding charge density plots of Be_2, Figure 4 of BHC. Figure 3 explains why this molecule is not bound. Since Be_2 falls between Li_2 and B_2, it is reasonable to expect that its total EMD would lie between these two molecules, if it indeed were bound. Figures 1 and 3 show clearly that this is not the case. In going from Li_2 to B_2 the contours become more elongated normal to the bond, especially the inner contours, but in Be_2 the corresponding contour lines are definitely elongated along the bond. It has been shown in the description of H_2 and He_2 in $\tilde{p}$-space (Ramirez 1982b) that He_2 is unbound because its electrons have momentum $\tilde{p}$ such that $p_z > p_x$, thus violating the "bond directional principle". This situation is clearly evident also in Be_2, and therefore it is unbound. The density difference map of Be_2 supports the conclusion that there is no positive $\Delta\rho$ that will

contribute to electrons having momentum $\tilde{p}$ such that $p_x > p_z$ upon molecular formation.

3. CONCLUDING REMARKS

Electron momentum density maps clearly provide another approach to the study of chemical binding in molecules. For the first-row homonuclear diatomic molecules, both the total EMD and density difference maps indicate that with the increasing tightness of the binding in the molecule ($Li_2 \rightarrow F_2$), there is a marked tendency for the electrons to move normal to, rather than along the bond axis, thereby confirming the "bond directional principle". It was also shown that Be_2 is unbound because its EMD distribution contradicts this principle; i.e., Be_2's EMD is elongated parallel to the bond axis. The last point appears to be clearer in momentum space than in position space.

ACKNOWLEDGMENTS

A post-doctoral fellowship from the Alexander von Humboldt Foundation and sponsorship by Professor Juergen Hinze at Universität Bielefeld are gratefully acknowledged. The author also expresses his thanks to Professor Abdus Salam, the IAEA and UNESCO for their hospitality at the International Centre for Theoretical Physics in Trieste, Italy.

REFERENCES

Bader RFW, Henneker WH and Cade PE 1967 J. Chem. Phys. 46 3341-3363

Cade PE and Wahl AC 1974 At. Data Nucl. Data Tables 13 339-551

Clementi C and Roetti C 1974 At. Data Nucl. Data Tables 14 177-478

Epstein IR and Tanner AC 1977 Compton Scattering ed. B. Williams (London: McGraw-Hill) 209-233

Henneker WH and Cade PE 1968 Chem. Phys. Lett. 2 575-578

Kaijser P and Smith VH 1976 Molec. Phys. 31 1557-1568

Matcha RL and Pettitt BM 1979 J. Chem. Phys. 70 3130-3132

Ramirez BI 1982a J. Phys. B: AT. Mol. Phys. (submitted for publication)

Ramirez BI 1982b ICTP Internal Report No. 124 (Trieste, Italy)

Table 1. Momentum density at the origin[a].

A_2	$\rho(A_2)$[b]	$\rho(A_2-2A)$[c]
Li_2	18.7836	1.6490
Be_2	4.9209	-6.9806
B_2	2.0360	-3.0341
C_2	0.9945	-0.0015
N_2	1.4079	-0.1906
O_2	0.9297	-0.0857
F_2	0.5883	-0.1007

[a] In units of electrons per a.u.^{3}. One a.u. of linear momentum = 1.9929×10^{-24} kg m s^{-1}.

[b] Total momentum density at the origin.

[c] Total momentum density difference (molecule - isolated atoms) at the origin.

FIGURE CAPTIONS

Figure 1. Total electron momentum density contour maps of the first-row homonuclear diatomic molecules. Here, as in the rest of the figures, p_x and p_z (chosen parallel to the diatomic axis) are in atomic units (1 a.u. of linear momentum = 1.9929×10^{-24} kg m s^{-1}). Contour values, in electrons per a.u.^{3}, starting from the outermost contour: 0.005, 0.006, 0.01, 0.02, 0.05, 0.10, 0.20, 0.50. The density at the origin is given in Table 1.

Figure 2. Total momentum density difference (molecule - isolated atoms) maps of the first-row homonuclear diatomic molecules. Solid contours and dash-dot contours represent positive and negative density difference regions, respectively. Contour values, in electrons per a.u.^{3}, for each set of contour lines with a common center, starting from the outermost contour: 0.0005, 0.001, 0.005, 0.01, 0.05, 0.10 for positive contours; -0.0005, -.001, -.005, -.01, -.05, -.10 for negative contours. The density at the origin is given in Table 1.

Figure 3. Total electron momentum density and momentum density difference maps for Be_2. Contour values same as in Figures 1 and 2. The density at the origin is given in Table 1.

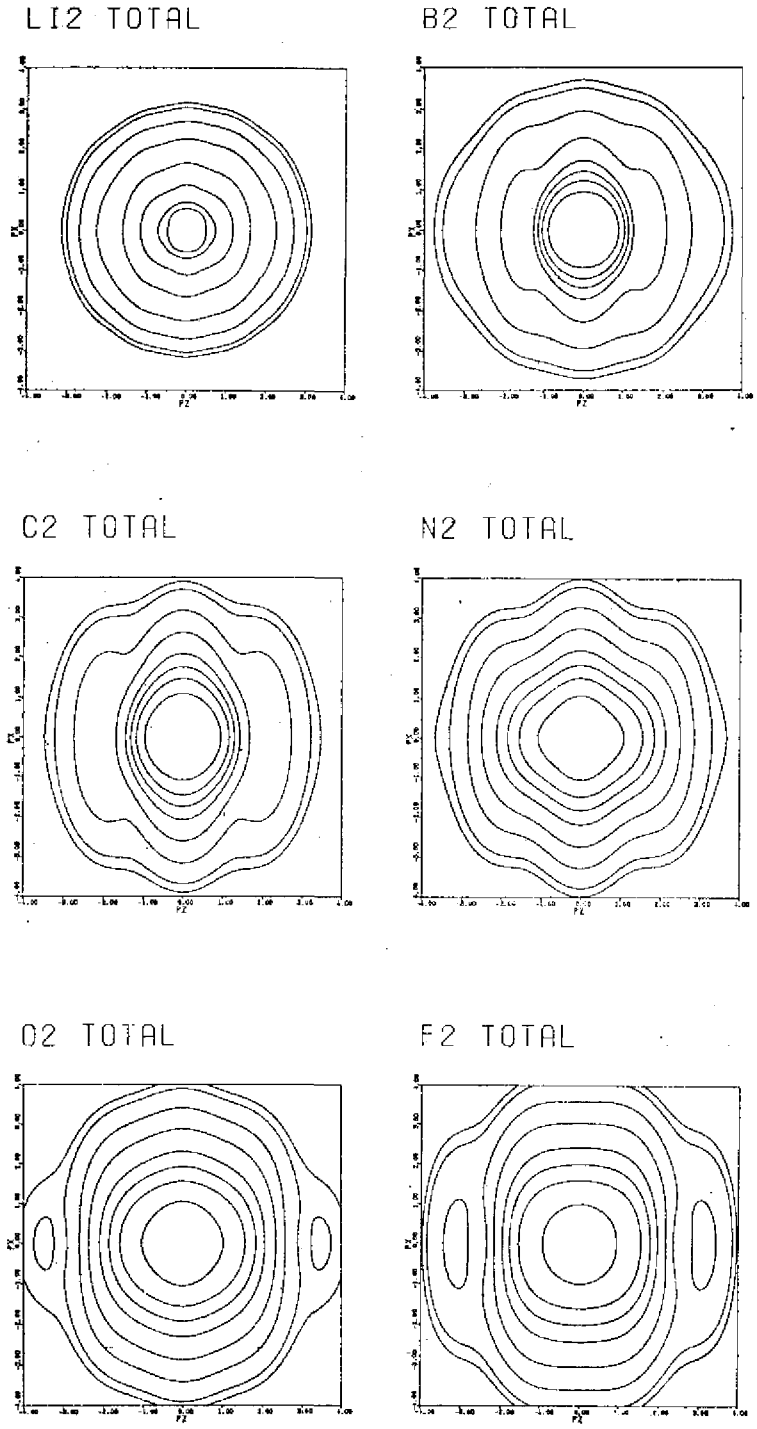

LI2-2LI

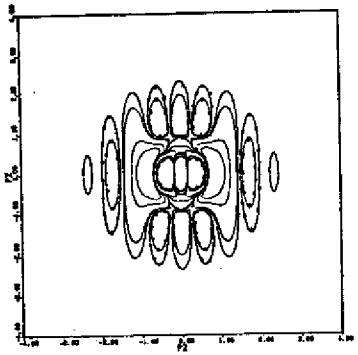

B2-2B

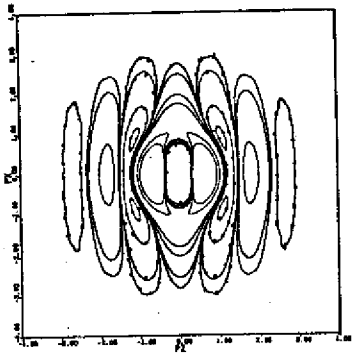

C2-2C

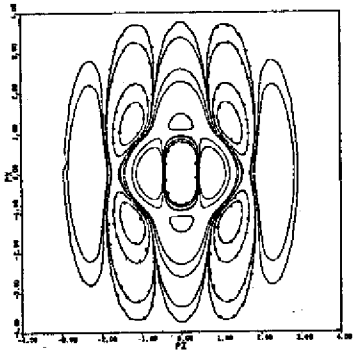

N2-2N

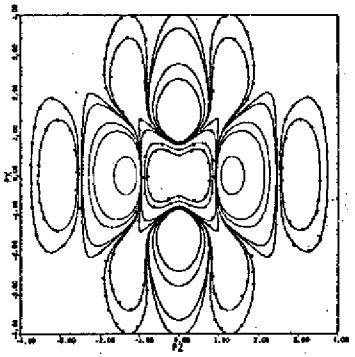

O2-2O

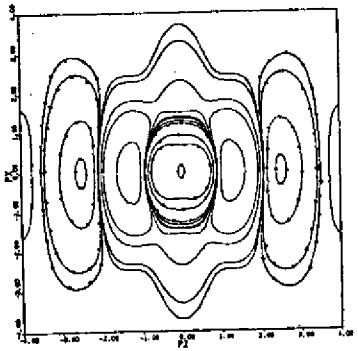

F2-2F

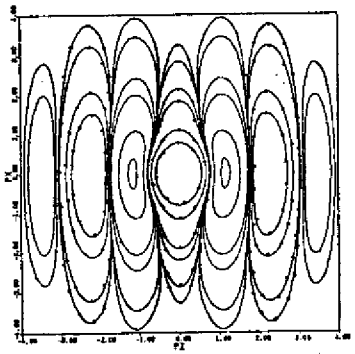

BE2 TOTAL

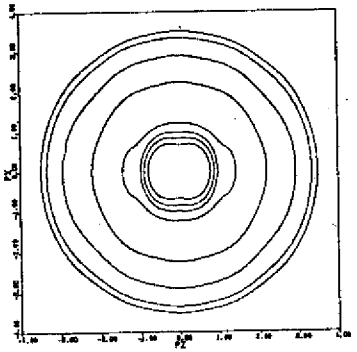

BE2-2BE

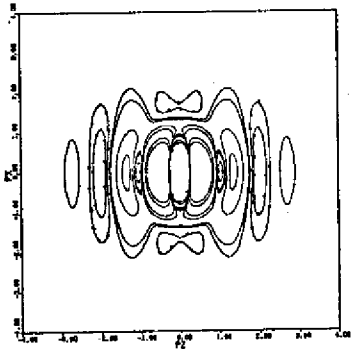

CURRENT ICTP PUBLICATIONS AND INTERNAL REPORTS

IC/82/23 INT.REP.* SUN KUN OH - Mass splitting between B^+ and B^0 mesons.

IC/82/24 INT.REP.* A. BREZINI - Self-consistent study of localization near band edges.

IC/82/25 INT.REP.* C. PANAGIOTAKOPOULOS - Dirac monopoles and non-Abelian gauge theories.

IC/82/26 CAO CHANG-qi and DING XING-fu - Intermediate symmetry $SU(4)_{EC} \times SU(2)_L \times U(1)_Y$ and the SU(N) unification series.

IC/82/27 H.B. GHASSIB and S. CHATTERJEE - ^{4}He-impurity effects on normal liquid ^{3}He at low temperatures - I: Preliminary ideas and calculations.

IC/82/28 C. PANAGIOTAKOPOULOS, ABDUS SALAM and J. STRATHDEE - Supersymmetric local field theory of monopoles.

IC/82/29 INT.REP.* G.A. CHRISTOS - Concerning the proofs of spontaneous chiral symmetry breaking in QCD from the effective Lagrangian point of view.

IC/82/30 INT.REP.* M.I. YOUSEF - Diffraction model analyses of polarized ^{6}Li elastic scattering.

IC/82/31 L. MIZRACHI - Electric-magnetic duality in non-Abelian gauge theories.

IC/82/32 INT.REP.* W. MECKLENBURG - Hierarchial spontaneous compactification.

IC/82/33 C. PANAGIOTAKOPOULOS - Infinity subtraction in a quantum field theory of charges and monopoles.

IC/82/34 INT.REP.* M.W. KALINOWSKI, M. SEWERYNSKI and L. SZYMANOWSKI - On the F equation.

IC/82/35 INT.REP.* H.C. LEE, LI BING-AN, SHEN QI-XING, ZHANG MEI-MAN and YU HONG - Electroweak interference effects in the high energy $e^+ + e^- \rightarrow e^+ + e^-$ + hadrons process.

IC/82/36 G.A. CHRISTOS - Some aspects of the U(1) problem and the pseudoscalar mass spectrum.

IC/82/37 C. MUKKU - Gauge theories in hot environments: Fermion contributions to one-loop.

IC/82/38 INT.REP.* W. KOTARSKI and A. KOWALEWSKI - Optimal control of distributed parameter system with incomplete information about the initial condition.

IC/82/39 INT.REP.* M.I. YOUSEF - Diffraction model analysis of polarized triton and ^{3}He elastic scattering.

IC/82/40 INT.REP.* S. SELZER and N. MAJLIS - Effects of surface exchange anisotropy in Heisenberg ferromagnetic insulators.

IC/82/41 INT.REP.* H.R. HAROON - Subcritical assemblies, use and their feasibility assessment.

IC/82/42 W. ANDREONI and M.P. TOSI - Why is AgBr not a superionic conductor?

THESE PREPRINTS ARE AVAILABLE FROM THE PUBLICATIONS OFFICE, ICTP, P.O. BOX 586, I-34100 TRIESTE, ITALY.

IC/82/43 N.S. CRAIGIE and J. STERN - What can we learn from sum rules for vertex functions in QCD?

IC/82/44 INT.REP.* ERNEST C. NJAU - Distortions in power spectra of digitised signals - I: General formulations.

IC/82/45 INT.REP.* ERNEST C. NJAU - Distortions in power spectra of digitised signals - II: Suggested solution.

IC/82/46 INT.REP.* H.R. DALAFI - A critique of nuclear behaviour at high angular momentum.

IC/82/47 N.S. CRAIGIE and P. RATCLIFFE - Higher power QCD mechanisms for large p_T strange or charmed baryon production in polarized proton-proton collisions.

IC/82/48 INT.REP.* B.R. BULKA - Electron density of states in a one-dimensional distorted system with impurities: Coherent potential approximation.

IC/82/49 INT.REP.* J. GORECKI - On the resistivity of metal-tellurium alloys for low concentrations of tellurium.

IC/82/50 S. RANDJBAR-DAEMI and R. PERCACCI - Spontaneous compactification of a (4+d)-dimensional Kaluza-Klein theory into $M_4 \times G/H$ for arbitrary G and H.

IC/82/51 INT.REP.* P.S. CHEE - On the extension of H^p-functions in polydiscs.

IC/82/53 INT.REP.* S. YOKSAN - Critical temperature of two-band superconductors containing Kondo impurities.

IC/82/54 M. ÖZER - More on generalized gauge hierarchies.

IC/82/55 N.S. CRAIGIE and P. RATCLIFFE - A simple method for isolating order α_S and α_S^2 corrections from polarized deep-inelastic scattering data.

IC/82/56 C. PANAGIOTAKOPOULOS - Renormalization of the QEMD of a dyon field.

IC/82/57 INT.REP.* J.A. MAGPANTAY - Towards an effective bilocal theory from QCD in a background.

IC/82/58 S. CHAKRABARTI - On stability domain of stationary solitons in a many-charge field model with non-Abelian internal symmetry.

IC/82/59 INT.REP.* J.K. ABOAYE and D.S. PAYIDA - High temperature internal friction in pure aluminium.

IC/82/60 Y. FUJIMOTO and ZHAO ZHIYONG - N-$\bar{N}$ oscillation in SO(10) and SU(6) supersymmetric grand unified models.

IC/82/61 J. GORECKI and J. POPIELAWSKI - On the application of the long mean free path approximation to the theory of electron transport properties in liquid noble metals.

IC/82/62 I.M. REDA, J. HAFNER, P. PONGRATZ, A. WAGENDRISTEL, H. BANGERT and P.K. BHAT - Amorphous Cu-Ag films with high stability.

IC/PD/82/1 INT.REP. PHYSICS AND DEVELOPMENT (Winter College on Nuclear Physics and Reactors, 25 January - 19 March 1982).